Role of high-spin hyperon resonances in the reaction of $\gamma p \to K^+K^+\Xi^-$

J. Ka Shing Man,[1] Yongseok Oh,[2,3,4,*] and K. Nakayama[1,5,†]
[1]*Department of Physics and Astronomy, University of Georgia, Athens, Georgia 30602, USA*
[2]*Department of Physics, Kyungpook National University, Daegu 702-701, Korea*
[3]*Excited Baryon Analysis Center, Thomas Jefferson National Accelerator Facility, Newport News, Virginia 23606, USA*
[4]*Asia Pacific Center for Theoretical Physics, POSTECH, Pohang 790-784, Korea*
[5]*Institut für Kernphysik, Forschungszentrum Jülich, D-52425 Jülich, Germany*
(Received 10 March 2011; published 6 May 2011)

The recent data taken by the CLAS Collaboration at the Thomas Jefferson National Accelerator Facility for the reaction of $\gamma p \to K^+K^+\Xi^-$ are reanalyzed within a relativistic meson-exchange model of hadronic interactions. The present model is an extension of the one developed in an earlier work by Nakayama, Oh, and Haberzettl [Phys. Rev. C **74**, 035205 (2006)]. In particular, the role of the spin-5/2 and -7/2 hyperon resonances, which were not included in the previous model, is investigated in the present study. It is shown that the contribution of the $\Sigma(2030)$ hyperon having spin-7/2 and positive parity has a key role to bring the model predictions into a fair agreement with the measured data for the $K^+\Xi^-$ invariant mass distribution.

DOI: 10.1103/PhysRevC.83.055201 PACS number(s): 25.20.Lj, 13.60.Le, 13.60.Rj, 14.20.Jn

I. INTRODUCTION

While there are extensive studies on the production of Λ and Σ hyperons [1–4], only a few attempts were made so far to understand the production of multistrangeness hyperons. In addition, the spectrum of multistrangeness hyperons is yet to be explored. For example, if the flavor SU(3) symmetry is good for the classification of baryons, we expect to have the number of Ξ resonances being equal to the sum of the number of nucleon resonances and the number of Δ resonances. However, while one can find more than 20 nucleon resonances and more than 20 Δ resonances in the review of particles compiled by the Particle Data Group (PDG), only a dozen or so Ξ's have been identified until today [5]. Furthermore, only two of them, $\Xi(1318)$ and $\Xi(1530)$, have four-star status according to the PDG. One of the reasons for this situation is that Ξ hyperons, being particles with strangeness $S = -2$, are difficult to produce as they have relatively small production rates. Namely, they can only be produced via indirect processes from the nucleon, which leads to very small production cross sections. It is, then, natural to see that the case of Ω hyperons is even worse.

The investigation on multistrangeness baryons, however, is expected to provide a very important tool to understand the structure of baryons and to distinguish various phenomenological models on baryon mass spectrum. In fact, most theoretical models on baryon spectrum could describe the mass spectra of the ground states of baryon octet and decuplet. However, this is basically a consequence of the group structure of the flavor SU(3) symmetry and the symmetry breaking terms. On the other hand, these models give very different predictions on the spectrum of excited states of hyperons. This high model dependence can be easily found in the spectrum of Ξ resonances. (See, e.g., Ref. [6].) In particular, description of the low-lying Ξ baryons, $\Xi(1620)$ and $\Xi(1690)$, would provide important insight to understanding baryon structure. Most quark models predict higher mass for the $\Xi(1690)$ and its predicted spin-parity quantum numbers depend on the details of the model [7–9]. Furthermore, the low mass of one-star-rated $\Xi(1620)$ is puzzling to quark models. On the other hand, these states were claimed to be dynamically generated S-wave resonances in unitarized meson-baryon interaction models [10,11]. In the bound-state approach to the Skyrme model, these states are described as bound states of the soliton and two kaons and, therefore, they are analogous to the $\Lambda(1405)$ [6]. Furthermore, in this model, the existence of the $\Xi(1620)$ is required as it accompanies the $\Xi(1690)$. Therefore, confirming the existence of Ξ resonances and verifying their quantum numbers will help shed light on the understanding of the multistrangeness baryon structure.

Experimentally, there have been several recent reports on the new measurements for the properties of Ξ weak decays [12,13] and for the Ξ resonances [14,15]. In particular, the BABAR Collaboration reported evidence of the spin-parity of the $\Xi(1690)$ being $\frac{1}{2}^-$ [16]. The investigation to understand the production mechanism of the ground-state Ξ baryon has been recently initiated by the CLAS Collaboration at the Thomas Jefferson National Accelerator Facility (TJNAF) [17–19]. It has established the feasibility to investigate hyperon spectroscopy via photoproduction reactions like $\gamma p \to K^+K^+\Xi^-$ and $\gamma p \to K^+K^+\pi^-\Xi^0$ [17,18]. The first dedicated experiment for these reactions has been carried out and the data for the total and differential cross sections as well as the K^+K^+ and $K^+\Xi^-$ invariant mass distributions for the $\gamma p \to K^+K^+\Xi^-$ reaction have been reported in Ref. [20]. To our knowledge, this is the first data set measured for the exclusive production of the Ξ in photon-nucleon scattering.

Theoretical investigation of the reaction mechanism of Ξ production has been started only recently [21–23]. The work of Ref. [21] was devoted to search for the pentaquark exotic Ξ hyperon, and the detailed analysis for the reaction of $\gamma N \to K K \Xi$ in the energy region up to ~ 4 GeV based on the data obtained at the TJNAF [20] was initiated by the work of

*yohphy@knu.ac.kr
†nakayama@uga.edu

Ref. [22]. In the present work, we extend the model of Ref. [22] to address the role of the contributions from the Λ and Σ hyperon resonances of spin-5/2 and -7/2 in the production mechanism.

The approach of Ref. [22] is based on a relativistic meson-exchange model of strong interactions and the reaction amplitude is calculated at the tree-level approximation by making use of an effective Lagrangian. As was discussed in Ref. [22], the main contribution to the reaction mechanisms of the $\gamma N \to KK\Xi$ reaction comes from the excitations of intermediate hyperons because of the absence of exotic mesons that have strangeness $S = +2$. (See Fig. 1.) This is the main difference from the reaction mechanism of the production of kaon and antikaon pair, i.e., $\gamma N \to K\bar{K}N$, which is dominated by the production of the ϕ meson [24]. Therefore, the reaction of Ξ photoproduction would be a very useful tool to investigate hyperons having $S = -1$.

In fact, there are number of three- and four-star Λ and Σ hyperon resonances [5] that may have a crucial role in the mechanism of Ξ production in the photon-nucleon scattering. Although their properties are not precisely determined yet, it has been explicitly shown in Ref. [22] that a potential contribution of hyperon resonances with a mass around 2 GeV can affect the $K^+\Xi^-$ invariant mass distribution in a significant way. The original model of Ref. [22], which includes only the lower mass hyperon resonances of spin-1/2 and -3/2, predicted a double-bump structure in the $K^+\Xi^-$ invariant mass distribution that was not exhibited by the observed data [19]. Instead, it was shown that a hyperon resonance of a mass around 2 GeV can fill the valley between the double bump to explain the experimental data. However, according to the PDG, there is no identified hyperon resonances of spin-1/2 or -3/2 in this mass region, but such resonances are found to have spin-5/2 or -7/2 [5]. (See Table I.)

It is, therefore, necessary to explore the role of the four-star spin-5/2 and -7/2 hyperons at a mass around 2 GeV in Ξ photoproduction by extending the model of Ref. [22]. It is the purpose of the present work, and here we concentrate on the photoproduction mechanism of the ground-state $\Xi(1318)$ off the proton target, i.e., $\gamma p \to K^+K^+\Xi^-$, where the data (including the $K^+\Xi^-$ invariant mass distribution) were collected by the CLAS Collaboration [20].

In the next section, we describe the extension of the original model of Ref. [22] for Ξ photoproduction, the dynamical content of which is shown in Fig. 1. We here include the contributions from the hyperon resonances of spin-5/2 and -7/2. Our results are then compared to the experimental data of the CLAS Collaboration [20] in Sec. III, focusing, in particular, on the role of the higher spin intermediate hyperons. Section IV contains a summary and discussions. Some details of the present model Lagrangian are given in the Appendix.

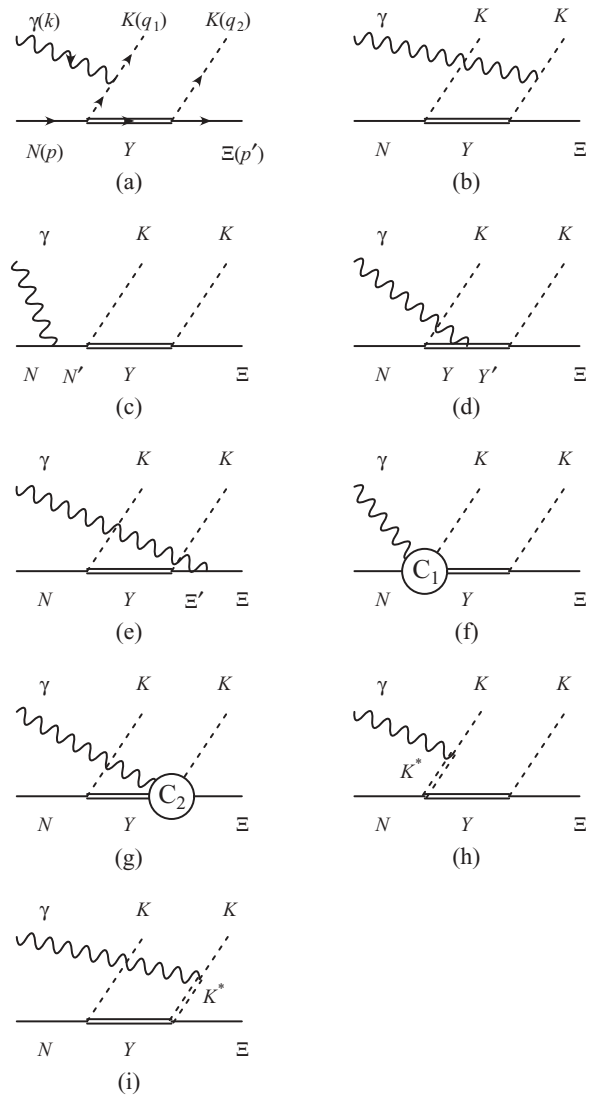

FIG. 1. Diagrams contributing to the reaction mechanism of $\gamma N \to KK\Xi$. The intermediate baryon states are denoted as N' for the nucleon and Δ resonances, Y, Y' for the Λ and Σ resonances, and Ξ' for $\Xi(1318)$ and $\Xi(1530)$. The intermediate mesons in the t channel are K [(a) and (b)] and K^* [(h) and (i)]. The diagrams (f) and (g) contain the generalized contact currents that maintain gauge invariance of the total amplitude. Diagrams corresponding to (a)–(i) with $K(q_1) \leftrightarrow K(q_2)$ are also understood.

II. MODEL FOR $\gamma p \to K^+K^+\Xi^-$

The model for describing the $\gamma p \to K^+K^+\Xi^-$ reaction in the present work is essentially the same as that of Ref. [22], which consists of the amplitudes shown in Fig. 1. The only difference is that here we include the spin-5/2 and -7/2 hyperons as will be specified below. Such high-spin resonances were not considered in the model of Ref. [22]. In the following, for completeness, we first discuss the most relevant features of the model of Ref. [22].

The three- and four-star hyperons that can contribute to the reaction of Ξ photoproduction are summarized in Table I. Among them, only for the low-mass resonances, i.e., $\Lambda(1116)$, $\Lambda(1405)$, $\Lambda(1520)$, $\Sigma(1190)$, and $\Sigma(1385)$, we have sufficient information to determine the relevant hadronic and electromagnetic coupling constants either from the experimental data [5] or from quark models with SU(3) symmetry consideration. These hyperon resonance parameters

TABLE I. Λ and Σ hyperons listed by the Particle Data Group [5] as three-star or four-star states. The decay widths and branching ratios of high-mass resonances $m_Y > 1.6$ GeV are in a broad range and the coupling constants are determined from their central values.

Λ states					Σ states				
State	J^P	Γ (MeV)	Rating	$\lvert g_{N\Lambda K}\rvert$	State	J^P	Γ (MeV)	Rating	$\lvert g_{N\Sigma K}\rvert$
Λ(1116)	$1/2^+$		****		Σ(1193)	$1/2^+$		****	
Λ(1405)	$1/2^-$	≈50	****		Σ(1385)	$3/2^+$	≈37	****	
Λ(1520)	$3/2^-$	≈16	****						
Λ(1600)	$1/2^+$	≈150	***	4.2	Σ(1660)	$1/2^+$	≈100	***	2.5
Λ(1670)	$1/2^-$	≈35	****	0.3	Σ(1670)	$3/2^-$	≈60	****	2.8
Λ(1690)	$3/2^-$	≈60	****	4.0	Σ(1750)	$1/2^-$	≈90	***	0.5
Λ(1800)	$1/2^-$	≈300	***	1.0	Σ(1775)	$5/2^-$	≈120	****	
Λ(1810)	$1/2^+$	≈150	***	2.8	Σ(1915)	$5/2^+$	≈120	****	
Λ(1820)	$5/2^+$	≈80	****		Σ(1940)	$3/2^-$	≈220	***	<2.8
Λ(1830)	$5/2^-$	≈95	****		Σ(2030)	$7/2^+$	≈180	****	
Λ(1890)	$3/2^+$	≈100	****	0.8	Σ(2250)	$?^?$	≈100	***	
Λ(2100)	$7/2^-$	≈200	****						
Λ(2110)	$5/2^+$	≈200	***						
Λ(2350)	$9/2^+$	≈150	***						

and the estimation of the corresponding coupling constants can be found in Ref. [22].

For higher-mass resonances (those listed in Table I with a mass larger than 1.6 GeV), however, there is no sufficient information to extract the necessary parameters, in particular, their coupling constants to the Ξ. The only available information relevant to the present reaction involving the higher hyperon resonances are their partial decay widths into the $N\bar{K}$ channel [5]. This information allows us to extract the magnitude of the corresponding NYK coupling constants, and their estimated values are displayed in Table I. Therefore, in Ref. [22], only the diagrams (a)–(g) in Fig. 1 with $Y = Y'$ in (d), where the only additional parameter is the ΞYK coupling constant, were considered, in addition to restricting Y to spin-1/2 and -3/2 hyperons.

It was then noted that, unless the ΞYK coupling constants are much larger than the corresponding NYK coupling constants, hyperon resonances with $J^P = 1/2^+$ and $3/2^-$ yield much smaller contributions to the reaction amplitude when compared to the $J^P = 1/2^-$ and $3/2^+$ resonance contributions. As was pointed out in Ref. [22], this can be understood by considering the intermediate hyperon resonance on its mass shell. By analyzing the production amplitude with an intermediate hyperon resonance on its mass shell, the photoproduction amplitude was found to be proportional to either the sum or difference of the baryon masses and energies depending on the spin-parity of the resonance, namely,[1]

$$\begin{aligned} |M_{1/2^\pm}|^2 &\propto (\varepsilon_N \mp m_N)\,(\varepsilon_\Xi \mp m_\Xi), \\ |M_{3/2^\pm}|^2 &\propto (\varepsilon_N \pm m_N)\,(\varepsilon_\Xi \pm m_\Xi), \end{aligned} \tag{1}$$

where M_{J^P} denotes the photoproduction amplitude involving the intermediate hyperon with the spin-parity J^P; $\varepsilon_i \equiv \sqrt{\boldsymbol{p}_i^2 + m_i^2}$, with $\boldsymbol{p}_i$ and m_i denoting the momentum and mass, respectively, of the nucleon or the Ξ as $i = N$ or Ξ. This proportionality is valid only when the intermediate hyperon lies on its mass shell, and it does not quite apply to the low-mass resonances, which are far off-shell in the present reaction. Among the $J^P = 1/2^-$ and $3/2^+$ resonances, assuming the ΞYK coupling strength to be of the order of the NYK coupling strength, only the $\Lambda(1800)1/2^-$ and $\Lambda(1890)3/2^+$ resonances contribute significantly.[2] Therefore, only these two high-mass resonances were considered in the model of Ref. [22].[3]

In the present work, we include the contributions from the spin-5/2 and -7/2 hyperon resonances to the model of Ref. [22], i.e., on top of the $\Lambda(1800)1/2^-$ and $\Lambda(1890)3/2^+$ resonances. This is motivated by the observation that the measured $K^+\Xi^-$ invariant mass distribution [20] exhibits no double-bump structure predicted by the model of Ref. [22] at around 2 GeV. In fact, one can find four-star spin-5/2 and -7/2 hyperons of this mass range in Table I and these resonances should be taken into account for understanding the production mechanism. By performing the similar analysis that lead to Eq. (1), we can obtain the analogous features for spin-5/2 and -7/2 resonances in the on-shell limit, which read

$$\begin{aligned} |M_{5/2^\pm}|^2 &\propto (\varepsilon_N \mp m_N)\,(\varepsilon_\Xi \mp m_\Xi), \\ |M_{7/2^\pm}|^2 &\propto (\varepsilon_N \pm m_N)\,(\varepsilon_\Xi \pm m_\Xi). \end{aligned} \tag{2}$$

This allows us to consider only the $J^P = 5/2^-$ and $7/2^+$ resonances. We then see from Table I that the $\Sigma(2030)7/2^+$, $\Sigma(1775)5/2^-$, and $\Lambda(1830)5/2^-$ are the only candidates. Among them, the $\Sigma(1775)5/2^-$ and $\Lambda(1830)5/2^-$ have a mass below or very close to the threshold. Since we are interested

[1]The error committed in Eq. (2) of Ref. [22] is corrected here. However, the results and the conclusions of Ref. [22] remain unchanged.

[2]For Λ resonances, one can expect $|g_{\Xi\Lambda K}/g_{N\Lambda K}| \leqslant 1$ since $g_{\Xi\Lambda K} = g_{N\Lambda K}$ for a singlet Λ and $g_{\Xi\Lambda K}/g_{N\Lambda K} = (1-4f)/(1+2f)$ for an octet Λ [25], which is less than 1 for $0 < f < 1$.

[3]Among the Σ resonances, the only candidate is the Σ(1750) with $J^P = 1/2^-$. However, it has a very small coupling constant $g_{N\Sigma K}$.

in the resonances of mass about 2 GeV, we focus on the role of the $\Sigma(2030)7/2^+$ resonances in the present work. In fact, we have verified explicitly that the inclusion of the spin-5/2 resonances mentioned above do not help eliminate the problem of the double-bump structure in the predicted $K^+\Xi^-$ invariant mass distribution mentioned in the Introduction.

The interaction Lagrangian and propagators of higher spin resonances that are needed to construct the respective production amplitudes [cf. diagrams (a)–(g) in Figs. 1 with $Y = Y'$ in (d) and $\Xi = \Xi'$ in (e)] are given in the Appendix. In this work, we adopt the pseudovector coupling for the interactions of spin-1/2 resonances with the nucleon and with the Ξ.

III. RESULTS

We now present the numerical results for the observables in the reaction of $\gamma p \to K^+K^+\Xi^-$. To be specific, as mentioned above, we adopt the pseudovector coupling for the meson couplings of spin-1/2 particles. As in Ref. [22], we include the $\Lambda(1800)\frac{1}{2}^-$ and $\Lambda(1890)\frac{3}{2}^+$ on top of the $\Lambda(1116)$, $\Lambda(1405)$, $\Lambda(1520)$, $\Sigma(1190)$, and $\Sigma(1385)$ hyperons. In addition, we include the hyperon resonances with masses around 2 GeV. Table I shows that there are several Λ and Σ resonances in this mass region, but most of them are expected to have small contributions according to our discussion in the previous section, as their spin-parity quantum numbers are $\frac{3}{2}^-$, $\frac{5}{2}^+$, and $\frac{7}{2}^-$. The only exception is the $\Sigma(2030)$ with the spin-parity of $\frac{7}{2}^+$. Therefore, to reduce the number of uncontrollable free parameters, we include only this resonance in the model of Ref. [22].

The propagator and effective Lagrangian of spin-7/2 resonance are given explicitly in the Appendix. It also contains those of spin-5/2 resonance for completeness. Since we are considering the reaction of $\gamma p \to K^+K^+\Xi^-$ in the present work, the intermediate hyperon resonance has neutral charge. Furthermore, we have no information on the magnetic moment of $\Sigma(2030)$ resonances. Therefore, we do not include the diagram of Fig. 1(d) corresponding to this resonance in the present calculation. The values of the free parameters used in the present calculation are given in Table II. The other parameter values of the model are given in Ref. [22].

TABLE II. Parameter values employed in the present calculation including the $\Sigma(2030)\frac{7}{2}^+$ resonance. The other parameter values are kept the same as given in Ref. [22].

Free parameters	Values
Signs of coupling constants:	
$g_{B\Lambda K}$ for $\Lambda(1405)$	0.91
$g_{\Xi\Lambda K}$ for $\Lambda(1405)$	0.91
$g_{\Lambda\Lambda'\gamma}$ for $\Lambda(1116) \leftrightarrow \Lambda(1520)$ transition	1.26
$g_{\Sigma\Lambda'\gamma}$ for $\Lambda(1193) \leftrightarrow \Lambda(1520)$ transition	2.22
Baryonic form factor:	
All exponents n	∞
Λ_B for p	1250 MeV
Λ_B for Ξ	1250 MeV
Λ_B for spin-1/2 hyperons	1250 MeV
Λ_B for spin-3/2 hyperons	1230 MeV
Λ_B for spin-7/2 hyperons	800 MeV
Product of coupling constants:	
$g_{N\Lambda K}g_{\Xi\Lambda K}$ for $\Lambda(1800)$	1.5
$g_{N\Lambda K}g_{\Xi\Lambda K}$ for $\Lambda(1890)$	2.0
$g_{N\Sigma K}g_{\Xi\Sigma K}$ for $\Sigma(2030)$	−4.2

Our results for the invariant mass distributions of the $K^+\Xi^-$ pair and the K^+K^+ pair are given in Fig. 2. In Fig. 2, the dot-dashed lines are the results of Ref. [22], where only the $\Lambda(1800)1/2^-$ and $\Lambda(1890)3/2^+$ are included on top of the low-lying resonances. In contrast to the experimental data from the CLAS Collaboration [20], this model yields a double-bump structure in the $K^+\Xi^-$ invariant mass distribution as illustrated in Fig. 2(a), which evidently shows that the contribution from a resonance with a mass around 2 GeV is missing. As can be seen by the dashed lines in Fig. 2(a), this can be attributed to the role of the $\Sigma(2030)$. When combined with the other terms,

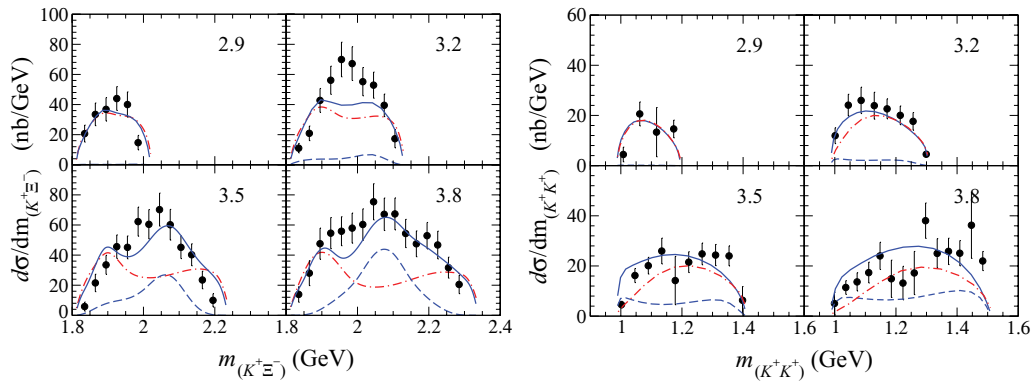

FIG. 2. (Color online) Invariant mass distribution (a) of the $K^+\Xi^-$ pair and (b) of the K^+K^+ pair in the reaction of $\gamma p \to K^+K^+\Xi^-$. The number in the right upper corner of each graph indicates the incident photon energy in GeV. The dot-dashed lines are the results of Ref. [22], which includes only spin-1/2 and -3/2 hyperon resonances. The solid lines are the results of the present model, while the dashed lines show the contributions from the $\Sigma(2030)7/2^+$. Experimental data are from Ref. [20].

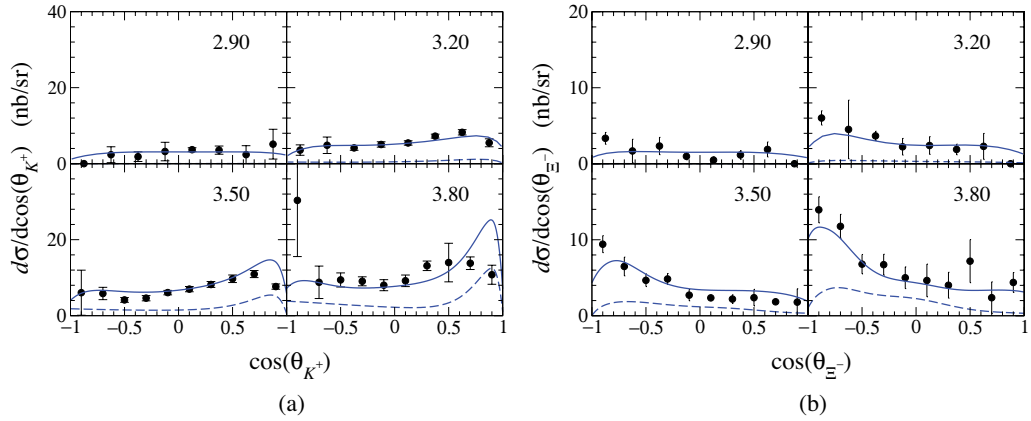

FIG. 3. (Color online) Differential cross section (a) $d\sigma/d\cos(\theta_{K^+})$ and (b) $d\sigma/d\cos(\theta_{\Xi^-})$ for $\gamma p \to K^+K^+\Xi^-$. The number in the right upper corner of each graph indicates the incident photon energy in GeV. The solid lines are the full results of the present model, while the dashed lines show the contributions from the $\Sigma(2030)7/2^+$. Experimental data are from Ref. [20].

the double-bump structure present in the model of Ref. [22] now disappears as shown by the solid lines in Fig. 2(a). This leads us to conclude that the $\Sigma(2030)$ of $J^P = \frac{7}{2}^+$ has a key role to bring the model predictions into a fair agreement with the CLAS data. As expected, the contribution from the $\Sigma(2030)7/2^+$ resonance can hardly be seen at low energies with $E_\gamma \leqslant 3.2$ GeV. Therefore, the results of the present model are very similar to those of the model of Ref. [22] at these energies. However, at higher energies, the range of the invariant $K^+\Xi^-$ mass fully covers the mass region of the $\Sigma(2030)$ and the results show the prominent contribution from this resonance.

Figure 2(b) shows the results for the invariant mass distribution of the K^+K^+ pair in the reaction of $\gamma p \to K^+K^+\Xi^-$. Here again, the contribution from the $\Sigma(2030)$ resonance is large for higher photon energies. However, as in the model of Ref. [22], the obtained K^+K^+ invariant mass distribution does not show any structure as expected from the absence of exotic $S = +2$ mesons.

In Fig. 3, we present the results for the differential cross sections $d\sigma/d\cos(\theta_{K^+})$ and $d\sigma/d\cos(\theta_{\Xi^-})$ for $\gamma p \to K^+K^+\Xi^-$. This again shows that the role of the $\Sigma(2030)$ becomes prominent as the incident photon energy increases and is crucial to reproduce the measured data for differential cross sections. In particular, $d\sigma/d\cos(\theta_{K^+})$ is forward peaked and $d\sigma/d\cos(\theta_{\Xi^-})$ is backward peaked, which supports the analyses of Ref. [22] and is verified by the experimental data. The contribution from the $\Sigma(2030)$ also respects this behavior.

IV. SUMMARY AND DISCUSSION

In the present paper, we have investigated the role of hyperon resonances with a mass around 2 GeV to understand the mechanism of Ξ^- photoproduction. Our model improves the previous one of Ref. [22] by including the $\Sigma(2030)$ as a high mass resonance. Since most of the resonances in this mass region have a spin higher than 5/2, we first developed a formalism for describing the interactions and decays of spin-5/2 and -7/2 resonances based on the Rarita-Schwinger formalism. Then, by analyzing the production amplitude near the mass shell, we found that the $J^P = \frac{5}{2}^-$ and $\frac{7}{2}^+$ resonances would have a nontrivial role in the production mechanism. In the mass region of 2 GeV, the only candidate among the hyperon resonances listed in the PDG is the $\Sigma(2030)$, and we have included this resonance in the present extended version of the model of Ref. [22]. In Ref. [22], a double-bump structure has been predicted in the $K^+\Xi^-$ invariant mass distribution in $\gamma p \to K^+K^+\Xi^-$, which is in marked discrepancy with the experimental data [20]. It has been suggested [22] that this discrepancy might be due to the missing of a resonance with a mass around 2 GeV. In this paper, we have explicitly shown that the $\Sigma(2030)$ has a crucial role in eliminating this double-bump structure.

Since there are many hyperon resonances that can contribute to Ξ^- photoproduction, the fitted coupling constants should be regarded as a very rough estimate and analyses based on more sophisticated models are required to obtain more reliable values for the resonance parameters, as well as more precise experimental data for various physical quantities of this reaction. However, our results show that the high-spin resonances, which have a mass of around 2 GeV, have a crucial role in the mechanism of Ξ^- photoproduction. In addition, the formalism for high-spin resonances discussed in the present work can be applied to analyze other reaction processes.

ACKNOWLEDGMENTS

We are grateful to L. Guo and T.-S. H. Lee for fruitful discussions. We also thank V. Pascalutsa and O. Scholten for discussions on high-spin fields. Y.O. is grateful to the Excited Baryon Analysis Center of the Thomas Jefferson National Accelerator Facility, where part of this work was done. We also acknowledge the University of Georgia Research Computing Center for providing the necessary computing resources. This work was supported by the FFE Grant No. 41788390 (COSY-58) and by Basic Science Research Program through the National Research Foundation of Korea (NRF) funded by the Ministry of Education, Science and Technology (Grant No. 2010-0009381).

APPENDIX: FORMALISM OF BARYON OF SPIN-5/2 AND -7/2

We refer the details for the interaction Lagrangian and propagators of spin-1/2 and -3/2 hyperons to Ref. [22]. Here we present our formalism for spin-5/2 and -7/2 hyperons.

A. Propagators

Following Refs. [26–28], we adopt the Rarita-Schwinger method to describe spin-5/2 and -7/2 baryon fields. Then the spin-5/2 field is described by a rank-2 tensor $R_{\mu\nu}$ and the spin-7/2 field by a rank-3 tensor $R_{\mu\nu\lambda}$. The propagators of the spin-5/2 and -7/2 fermion fields are written as

$$S_{5/2}(p) = \frac{i}{\not{p} - m_R + i\Gamma/2}\Delta^{\beta_1\beta_2}_{\alpha_1\alpha_2},$$
$$S_{7/2}(p) = \frac{i}{\not{p} - m_R + i\Gamma/2}\Delta^{\beta_1\beta_2\beta_3}_{\alpha_1\alpha_2\alpha_3}, \tag{A1}$$

where m_R and Γ are the mass and the decay width of the resonance, respectively. The spin projection operators are obtained by [29]

$$\sum_{\text{spins}} R_{\alpha_1\alpha_2\ldots}\bar{R}^{\beta_1\beta_2\cdots} = \Lambda_{\pm}\Delta^{\beta_1\beta_2\cdots}_{\alpha_1\alpha_2\ldots}, \tag{A2}$$

where $\Lambda_{\pm}$ are the usual energy projection operators of the spin-1/2 theory. Explicitly, they are obtained as [26–28]

$$\Delta^{\beta_1\beta_2}_{\alpha_1\alpha_2}\left(\frac{5}{2}\right) = \frac{1}{2}\left(\theta^{\beta_1}_{\alpha_1}\theta^{\beta_2}_{\alpha_2} + \theta^{\beta_2}_{\alpha_1}\theta^{\beta_1}_{\alpha_2}\right) - \frac{1}{5}\theta_{\alpha_1\alpha_2}\theta^{\beta_1\beta_2} - \frac{1}{10}\left(\bar{\gamma}_{\alpha_1}\bar{\gamma}^{\beta_1}\theta^{\beta_2}_{\alpha_2} + \bar{\gamma}_{\alpha_1}\bar{\gamma}^{\beta_2}\theta^{\beta_1}_{\alpha_2} + \bar{\gamma}_{\alpha_2}\bar{\gamma}^{\beta_1}\theta^{\beta_2}_{\alpha_1} + \bar{\gamma}_{\alpha_2}\bar{\gamma}^{\beta_2}\theta^{\beta_1}_{\alpha_1}\right),$$
$$\Delta^{\beta_1\beta_2\beta_3}_{\alpha_1\alpha_2\alpha_3}\left(\frac{7}{2}\right) = \frac{1}{36}\sum_{P(\alpha),P(\beta)}\left(\theta^{\beta_1}_{\alpha_1}\theta^{\beta_2}_{\alpha_2}\theta^{\beta_3}_{\alpha_3} - \frac{3}{7}\theta^{\beta_1}_{\alpha_1}\theta_{\alpha_2\alpha_3}\theta^{\beta_2\beta_3} - \frac{3}{7}\bar{\gamma}_{\alpha_1}\bar{\gamma}^{\beta_1}\theta^{\beta_2}_{\alpha_2}\theta^{\beta_3}_{\alpha_3} + \frac{3}{35}\bar{\gamma}_{\alpha_1}\bar{\gamma}^{\beta_1}\theta_{\alpha_2\alpha_3}\theta^{\beta_2\beta_3}\right), \tag{A3}$$

where

$$\theta^{\nu}_{\mu} = g^{\nu}_{\mu} - \frac{p_\mu p^\nu}{M^2}, \quad \bar{\gamma}_\mu = \gamma_\mu - \frac{p_\mu \not{p}}{M^2}, \tag{A4}$$

with M being the resonance mass. In Eq. (A3), the propagator for the spin-7/2 field contains summation over all possible permutations of $\{\alpha_1, \alpha_2, \alpha_3\}$ and $\{\beta_1, \beta_2, \beta_3\}$.

B. Effective Lagrangian

By considering parity and angular momentum conservation, one can easily confirm that there is only one form factor in the interaction of a hyperon of arbitrary spin with the nucleon-kaon channel or with the Ξ-kaon channel. By introducing

$$\Gamma^{(\pm)} = \begin{pmatrix} \gamma_5 \\ 1 \end{pmatrix}, \tag{A5}$$

and dropping the isospin dependence, the interaction Lagrangian of spin-5/2 hyperon field $Y_{\mu\nu}$ reads

$$\mathcal{L}^{5/2^\pm}_{BYK} = i\frac{g_{BYK}}{m_K^2}\bar{B}\Gamma^{(\pm)}Y^{\mu\nu}\partial_\mu\partial_\nu\bar{K} + \text{H.c.},$$
$$\mathcal{L}^{5/2^\pm}_{BYK\gamma} = -\frac{g_{BYK}}{m_K^2}\hat{e}_K\bar{B}\Gamma^{(\pm)}Y^{\mu\nu}(A_\mu\partial_\nu + \partial_\nu A_\nu)\bar{K} + \text{H.c.}, \tag{A6}$$

where the latter is obtained from the former by minimal substitution. Here, $\hat{e}_K$ is the charge of the K meson.

The corresponding Lagrangians for a spin-7/2 resonance are given by

$$\mathcal{L}^{7/2^\pm}_{BYK} = -\frac{g_{BKY}}{m_K^3}\bar{B}\Gamma^{(\mp)}Y^{\mu\nu\alpha}\partial_\mu\partial_\nu\partial_\alpha K + \text{H.c.},$$
$$\mathcal{L}^{7/2^\pm}_{BYK\gamma} = i\frac{g_{BYK}}{m_K^3}\bar{B}\Gamma^{(\pm)}Y^{\mu\nu}\hat{e}_K A_{\mu\nu}\bar{K} + \text{H.c.} \tag{A7}$$

[1] R. Bradford *et al.* (CLAS Collaboration), Phys. Rev. C **73**, 035202 (2006).
[2] R. G. T. Zegers *et al.*, Phys. Rev. Lett. **91**, 092001 (2003).
[3] SAPHIR Collaboration, M. Q. Tran *et al.*, Phys. Lett. B **445**, 20 (1998).
[4] K. Tsukada *et al.*, Phys. Rev. C **78**, 014001 (2008).
[5] Particle Data Group, K. Nakamura *et al.*, J. Phys. G **37**, 075021 (2010) [http://pdg.lbl.gov].
[6] Y. Oh, Phys. Rev. D **75**, 074002 (2007).
[7] K.-T. Chao, N. Isgur, and G. Karl, Phys. Rev. D **23**, 155 (1981).
[8] S. Capstick and N. Isgur, Phys. Rev. D **34**, 2809 (1986).
[9] M. Pervin and W. Roberts, Phys. Rev. C **77**, 025202 (2008).
[10] A. Ramos, E. Oset, and C. Bennhold, Phys. Rev. Lett. **89**, 252001 (2002).
[11] C. García-Recio, M. F. M. Lutz, and J. Nieves, Phys. Lett. B **582**, 49 (2004).
[12] E. Abouzaid *et al.* (KTeV Collaboration), Phys. Rev. Lett. **95**, 081801 (2005).
[13] NA48/1 Collaboration, J. R. Batley *et al.*, Phys. Lett. B **645**, 36 (2007).
[14] Belle Collaboration, K. Abe *et al.*, Phys. Lett. B **524**, 33 (2002).
[15] R. Witt *et al.* (STAR Collaboration), J. Phys. G **34**, S921 (2007).

[16] B. Aubert *et al.* (BABAR Collaboration), Phys. Rev. D **78**, 034008 (2008).
[17] J. W. Price *et al.* (CLAS Collaboration), Phys. Rev. C **71**, 058201 (2005).
[18] J. W. Price, J. Ducote, J. Goetz, and B. M. K. Nefkens (CLAS Collaboration), Nucl. Phys. A **754**, 272c (2005).
[19] CLAS Collaboration, L. Guo and D. P. Weygand, in *Proceedings of International Workshop on the Physics of Excited Baryons (NSTAR 05)*, edited by S. Capstick, V. Crede, and P. Eugenio (World Scientific, Singapore, 2006), pp. 384–388.
[20] L. Guo *et al.* (CLAS Collaboration), Phys. Rev. C **76**, 025208 (2007).
[21] W. Liu and C. M. Ko, Phys. Rev. C **69**, 045204 (2004).
[22] K. Nakayama, Y. Oh, and H. Haberzettl, Phys. Rev. C **74**, 035205 (2006).
[23] Y. Oh, H. Haberzettl, and K. Nakayama, Nucl. Phys. A **790**, 498 (2007); K. Nakayama, Y. Oh, and H. Haberzettl, J. Phys. Conf. Ser. **69**, 012023 (2007).
[24] Y. Oh, K. Nakayama, and T.-S. H. Lee, Phys. Rep. **423**, 49 (2006).
[25] J. J. de Swart, Rev. Mod. Phys. **35**, 916 (1963); **37**, 326(E) (1965).
[26] R. E. Behrends and C. Fronsdal, Phys. Rev. **106**, 345 (1957).
[27] J. G. Rushbrooke, Phys. Rev. **143**, 1345 (1966).
[28] S.-J. Chang, Phys. Rev. **161**, 1308 (1967).
[29] C. Fronsdal, Suppl. Nuovo Cimento **9**, 416 (1958).